Proceedings of the 17th World Congress
The International Federation of Automatic Control
Seoul, Korea, July 6-11, 2008

Wind turbine modeling by friction effects

Juvenal Villanueva * **Luis Alvarez-Icaza** **

* *Instituto de Ingeniería, Universidad Nacional Autónoma de México, 04510 Coyoacán, DF MEX; jvillanuevama@iingen.unam.mx*
** *Instituto de Ingeniería, Universidad Nacional Autónoma de México, 04510 Coyoacán, DF MEX; alvar@pumas.iingen.unam.mx*

Abstract The mechanical power in a wind turbine is modeled from a friction phenomenon perspective. Two models for the available power are derived based on a relative speed between the wind and turbine blades. The models are compared with a heuristic reference model showing good performance.

Keywords: wind power, friction models, wind turbines, modeling

1. INTRODUCTION

Including renewable energy sources as a larger component in electric power supply systems has become very important in recent years. The use of wind turbines to extract the kinetic energy of the air is one of the technologies with fastest growth (Danish [2003]). The main goal in a wind turbine is to maximize the power extracted from the wind, under safe operation constraints. The use of appropiate control techniques plays a key role in the conversion and safe extraction of the available power in the wind.

In the literature, there are different methods for the design of controllers to improve the wind turbine's performance (see, for example, Lin and Qingding [2003], Lima et al. [1999], Balas et al. [2003], Song et al. [2000], Dadone and Dambrosio [2003]). Most of them use a heuristic model for the mechanical power (P) or the performance coefficient (C_p), like the one proposed in Heier [1998], that is given by

$$P = \frac{1}{2}\,\rho\, C_p(\lambda, \alpha)\, A_R\, \dot{x}^3 \ , \tag{1}$$

with

$$C_p = 0.5\left(\frac{116}{\lambda_i} - 0.4\alpha - 5\right) e^{-\frac{21}{\lambda_i}} \ , \tag{2}$$

$$\frac{1}{\lambda_i} = \left(\frac{1}{\lambda + 0.08\alpha} - \frac{0.035}{\alpha^3 + 1}\right) \ , \tag{3}$$

$$\lambda = \frac{R\omega}{\dot{x}} \ , \tag{4}$$

where

- A_R is the area covered by the blades during rotation
- C_p is the performance coefficient of the turbine
- $\dot{x}$ is the wind speed
- ρ is the air density
- λ is the tip speed ratio of the rotor blade
- α is the blade pitch angle
- R is the ratio of blades
- ω is the angular velocity of the turbine rotor

In Fig. 1, the characteristic curves of the performance coefficient (C_p) are shown, for several values of the α, the blades pitch angle. As can be appreciated from Eqs. (1)-(4), the performance coefficient in Eq. (2) is the most complex term in the model. The highly nonlinear structure of the model makes it difficult to precisely find the value of its parameters. The complexity of the model structure makes it not possible the use of efficient parametric identification methods.

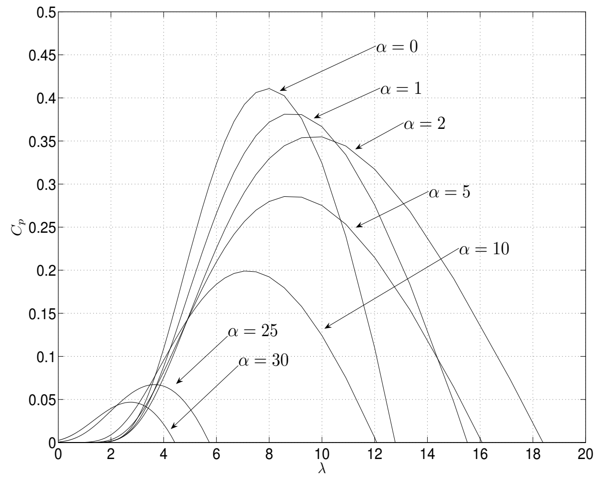

Figure 1. Characteristic curves of C_p vs λ, for different blade pitch angles.

In this paper, an alternative model for the power of the wind turbine is proposed. The model is developed around the hypothesis that a wind turbine is basically a device that works based on the friction effect between the wind and the turbine blades. The goal is to develop a model that has physical grounds and is easier to use and callibrate for control purposes.

In order to develop this new model, in section 2 a transformation of the performance coefficient in terms of a relative velocity between the wind speed and the turbine blades is introduced. The mechanical power of the wind turbine, written in terms of this relative velocity, is analyzed in section 3. Section 4 presents two models for the mechanical power, including simulation results that compare the new models with that in Eqs. (1)-(4). Finally, section 5 includes concluding remarks and proposes future work.

2. COORDINATE TRANSFORMATION OF THE PERFORMANCE COEFFICIENT MODEL

The possibility of extracting kinetic energy from the wind is related with some notion of an average relative velocity between the wind and the blades. The actual definition of the tip speed ratio, the main element to determine the behavior of the performance coefficent in Eq. (2), does not incorporate any use of relative speed. This can be easily observed when the behavior of the model in Eqs. (1)-(4) is applied for large values of tip speed ratio λ. In this situation, the model yields a negative performance coefficient that corresponds to the expected behavior when blades are acting as a fan and not as a turbine. However, the shape of this approximation does not follow the symmetric behavior that is expected when this turbine-fan transition occurs. This happens because the heuristic model in Eqs. (1)-(4) was developed to describe only the turbine behavior, and, in general, it is not valid for negative values of the performance coefficient.

The goal is to transform the tip speed ratio into a new variable that dependes on a relative velocity. For that purpose define a normalized relative velocity $\lambda' \in \Re$ as

$$\lambda' = \frac{\dot{x} - r\omega}{\dot{x}_m}, \quad \dot{x}_m \neq 0, \tag{5}$$

where $\dot{x}_m$ is the medium speed of the wind and r is an equivalent radius ($r \neq R$) that is to be determined. Solving Eqs. (4) and (5) for ω and equating

$$\lambda = \frac{R}{r}\left[1 - \lambda' \frac{\dot{x}_m}{\dot{x}}\right]. \tag{6}$$

Solving Eq. (6) for λ' yields

$$\lambda' = \frac{\dot{x}}{\dot{x}_m}\left[1 - \lambda\frac{r}{R}\right], \tag{7}$$

Assuming that $\dot{x}_m$, $\dot{x}$ and R are known, r is the variable that relates λ and λ'. To find r, postulate that there should be no power if there is not relative velocity. Equivalently, when the relative velocity coordinate vanishes, $\lambda' = 0$, the performance coefficient should also vanish $C_p = 0$, that is

$$C_p = 0 \quad \Leftrightarrow \quad \lambda' = 0. \tag{8}$$

From Eqs. (2) and (8) it follows that

$$0.5\left(\frac{116}{\lambda_i} - 0.4\alpha - 5\right)e^{-\frac{21}{\lambda_i}} = 0. \tag{9}$$

From the parenthesis in Eq. (9) it follows that

$$\frac{1}{\lambda_i} = \frac{0.4\alpha + 5}{116}. \tag{10}$$

Equating (3) and (10) yields

$$\lambda = \frac{1}{\dfrac{0.4\alpha + 5}{116} + \dfrac{0.035}{\alpha^3 + 1}} - 0.08\alpha. \tag{11}$$

Finally, from Eqs. (6) and (11) it is possible to write

$$r = R\left[\frac{(0.4\alpha + 5) + \dfrac{4.06}{\alpha^3 + 1}}{116 - 0.08\alpha\Big((0.4\alpha + 5) + \dfrac{4.06}{\alpha^3 + 1}\Big)}\right], \tag{12}$$

the value of the equivalent radius, r, as a function of α, the blade angle. Finally

$$C_p = sgn(\lambda')0.5\left(\frac{116}{\lambda_i} - 0.4\alpha - 5\right)e^{-\frac{21}{\lambda_i}}, \tag{13}$$

that now depends on Eqs. (5), (6) (3), and (12). The function sgn extracts the sign of its argument.

Fig. 2 shows the characteristic curves of the new model. In this new representation, it is possible to note the symmetry of the model around the zero relative velocity, that separates the turbine and fan modes of operation.

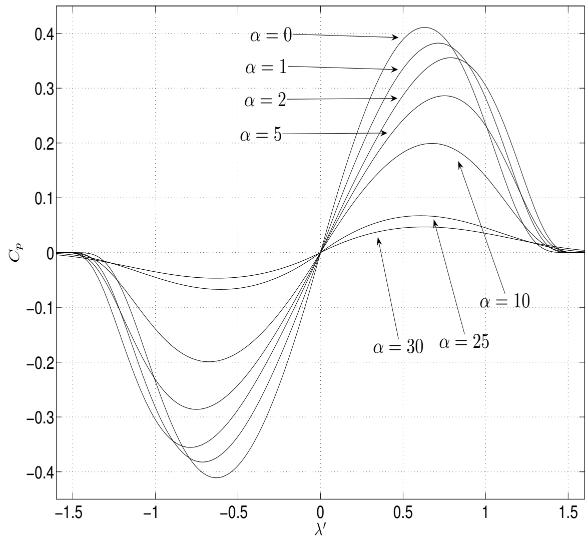

Figure 2. Characteristic curves of C_p vs λ'.

3. MECHANICAL POWER OF A WIND TURBINE

The interest in controlling a wind turbine is directly related with the power that can be extracted from the wind. For this reason in this section a model that directly models the power in the turbine is introduced. This model follows from the behavior in terms of relative velocity introduced in the previous section. Consider first a definition of relative speed based on the external radius of the blades given by

$$\dot{x}_R = \dot{x} - R\omega. \tag{14}$$

Fig. 3 shows the value of power P against this relative velocity, $\dot{x}_R$, for different values of the angular velocity, ω, obtained from Eqs. (1) and (13).

From Fig. 3, it can be observed that if $P = 0$ then $\dot{x}_R \neq 0$, and that the value of $\dot{x}_R$ at the zero power points is different for each ω. A new relative velocity, $\dot{x}_{r'}$, is needed such that

$$P = 0 \Longleftrightarrow \dot{x}_{r'} = 0, \tag{15}$$

where

$$\dot{x}_{r'} = \dot{x} - r'\omega, \tag{16}$$

as $\dot{x}$ and ω are known, r' must satisfy

$$\dot{x} - r'\omega = 0 \Longleftrightarrow P = 0, \tag{17}$$

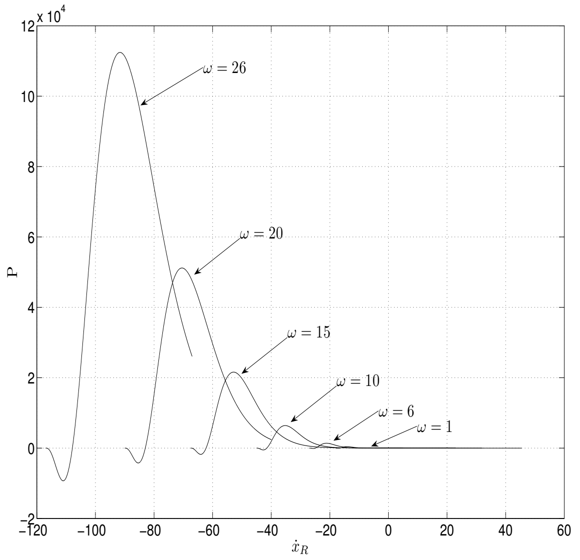

Figure 3. Mechanical power vs relative speed, $\dot{x}_R$, for different values of ω.

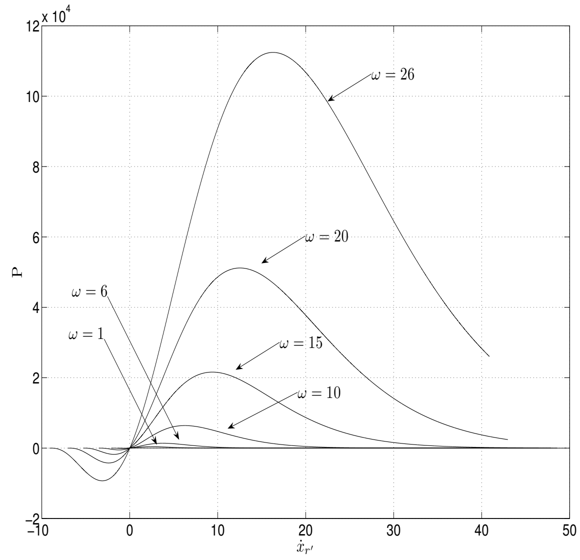

Figure 4. Mechanical power vs relative speed, $\dot{x}_{r'}$, for different values of ω.

or equivalently

$$r' = \frac{\dot{x}}{\omega}. \tag{18}$$

If the values of $\dot{x}$ and ω are evaluated for all points when $P = 0$, the obtained value is $r' = 0.078 \times R$ for all cases [1]. This result confirms that the hypothesis of the influence of the relative velocity is essentially correct. Fig. 4 shows the plots of P versus $\dot{x}_{r'}$ for different values of ω. It can be easily appreciated that the resulting curves in this figure have a similar behavior, in terms of symmetry, that the curves of the transformed C_p shown in Fig. 2. In this case the turbine operation mode is on the right hand side of the zero crossing and the fan mode of operation is on the other side.

4. TWO MODELS FOR THE MECHANICAL POWER OF THE WIND TURBINE

The power curves in Fig. 4 will be used as a reference value to propose two models in terms of relative velocity. These two models are restricted for the case of positive relative velocity, that is when $sgn(\dot{x}_{r'}) = 1$. Similar models can be derived for the case of negative relative velocity.

4.1 Model with 3 parameters

The first proposed model is given by

$$P = k_1 e^{-k_2 \dot{x}_{r'}} \dot{x}_{r'}^{k_3} \dot{x}^3, \tag{19}$$

where k_1, k_2 and k_3 are parameters to be found. This model was inspired by the shape of curves in Fig. 4 and the work in Yi et al. [2002]. It is straightforward to show that the following parameterization holds

$$ln\left(\frac{P}{\dot{x}^3}\right) = [1 \quad \dot{x}_{r'} \quad ln(\dot{x}_{r'})][\sigma_0 \quad \sigma_1 \quad \sigma_2]^T,$$

[1] The value was obtained for the case study with $R = 6$ m is, therefore, $r' = 0.078 \times R = 0.47$.

where the vector of parameters is given by

$$\Sigma = \begin{bmatrix} \sigma_0 \\ \sigma_1 \\ \sigma_2 \end{bmatrix} = \begin{bmatrix} ln(k_1) \\ -k_2 \\ k_3 \end{bmatrix},$$

and the regressor is

$$\Phi = [1 \quad \dot{x}_{r'} \quad ln(\dot{x}_{r'})].$$

Therefore, P can be expressed as

$$ln(\frac{P}{\dot{x}^3}) = \Phi\Sigma, \tag{20}$$

Eq. (20) allows to directly use a standard least squares algorithm with normalization (see, for example, Ioannou and Sun [1996]). To test this model against the reference model in the power curves of Fig. 4 a simulation was carried out with the following data

- $R = 6$ m.
- $\dot{x}_m = 15$ m/s.
- $\alpha = 0$.
- $\rho = 1.225$ kg/m^3.
- $\omega \in [1, 12]$ Hz.

As excitation signal, the wind speed plotted in Fig. 5 was used. Results of the least squares estimation are shown in Fig. 6, only for $\omega = 1, 7, 12$. The final estimation error for the worst case, that corresponds to $\omega = 12$, is of 2.5%.

Fig. 7 shows the time evolution of parameters, for the same values of ω used in Fig. 6. It can be easily observed that parameters have a fast convergence. Fig. 8 shows the value of the parameter plotted against variations of ω, the rotor angular speed. It is very clear that a particular set of parameters is only valid for a given ω.

4.2 Model with 4 parameters

The second model proposed is given by

$$P = \sigma_0 + \sigma_1 \dot{x}_{r'} + \sigma_2 \dot{x}_{r'}^{1,5} + \sigma_3 \dot{x}_{r'}^2, \tag{21}$$

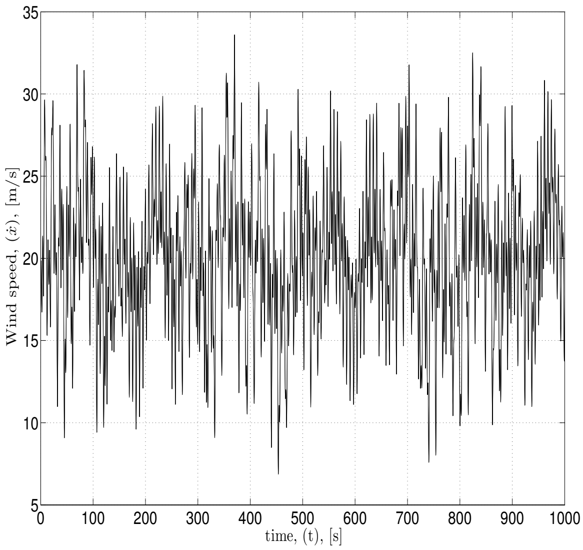

Figure 5. Wind speed vs time.

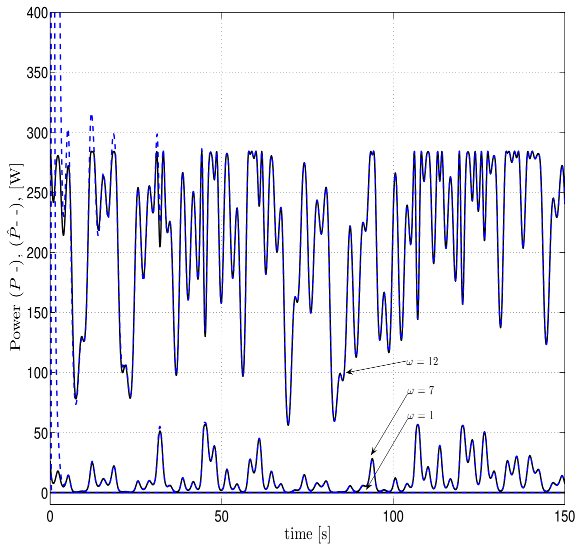

Figure 6. Mechanical Power vs time, for the three parameters model. Reference: solid, estimated: dotted

that is inspired by the form of the force on some dynamic friction models (see Canudas de Wit et al. [1995], for example). Its parameters can be arranged as follows

$$P = [1 \quad \dot{x}_{r'} \quad \dot{x}_{r'}^{1.5} \quad \dot{x}_{r'}^{2}][\sigma_0 \quad \sigma_1 \quad \sigma_2 \quad \sigma_3]^T. \tag{22}$$

Two simulations were performed. In the first case, the same data that in the previous subsection is used, $\alpha = 0$ and ω in the range of $[1, 12]$. This allows to compare the results for both models. In the second case, the angular velocity was fixed to $\omega = 6$ and the blades angle was evaluated for $\alpha \in [0, 30]$.

Case 1: α = cte. Fig. 9 shows the results of the estimation for the power with the model in Eq. (21) and values of $\omega = 1, 7, 12$. It is clear that the obtained estimation errors are smaller than those obtained with the three parameters model in Eq. (21). Again the maximum error occurs for $\omega = 12$ and its size is about 1.4%, more than 40% smaller than in the previous case.

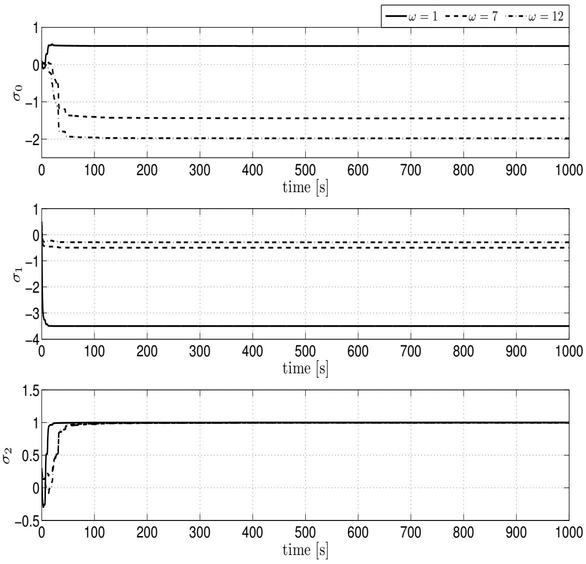

Figure 7. Parameters σ_i versus time for the three parameters model.

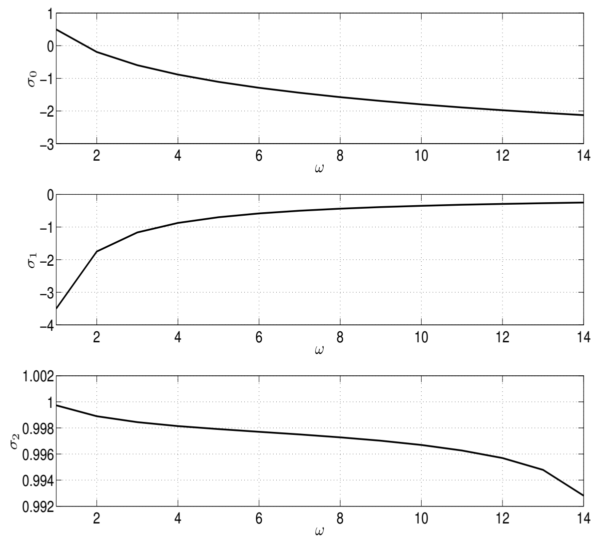

Figure 8. Parameters σ_i versus ω for the three parameters model.

Fig. 10 shows the time evolution of the parameters, that confirms rapid convergence. Fig. 11 plots the behavior of the final parameters σ_i against the angular velocity ω. The curves have now a more complex shape.

Case 2: ω = cte. This case was analyzed to cope with situations when the wind turbine is coupled with a synchronous electrical machine. Here the angular velocity is kept constant and the blades angle is changed. The estimation was performed for $\omega = 6$ and $\alpha \in [0, 30]$. The power model identification results, for values of $\alpha =$

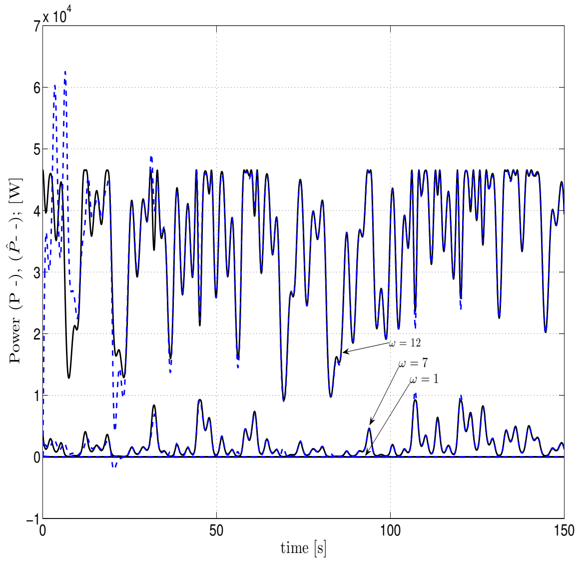

Figure 9. Mechanical power versus time, for the four parameters model. Reference: solid, estimated: dotted. Case 1: $\alpha = 0$ and ω= 1, 7, 12.

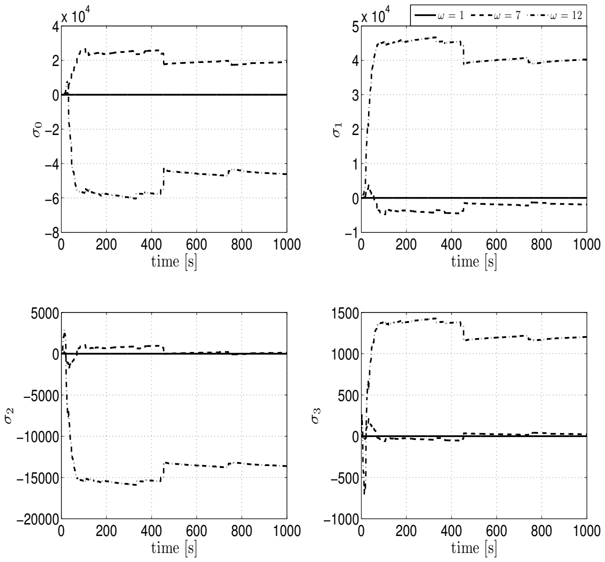

Figure 10. Time evolution of identified parameters for the four parameters model. Case 1: $\alpha = 0$

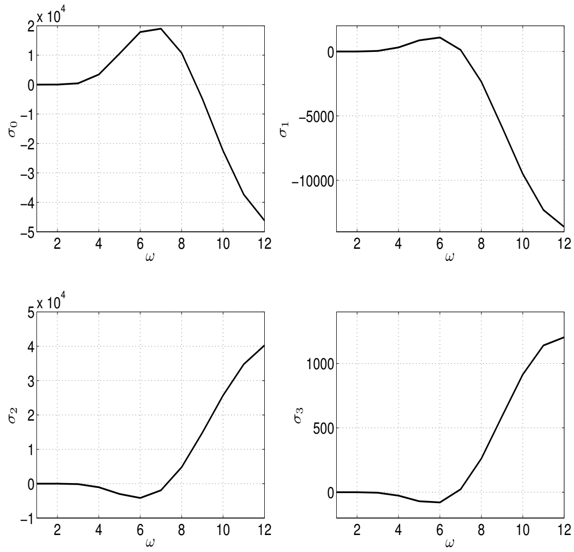

Figure 11. Final parameter estimation versus ω for the four parameters model. Case 1: $\alpha = 0$ and ω= 1, 7, 12.

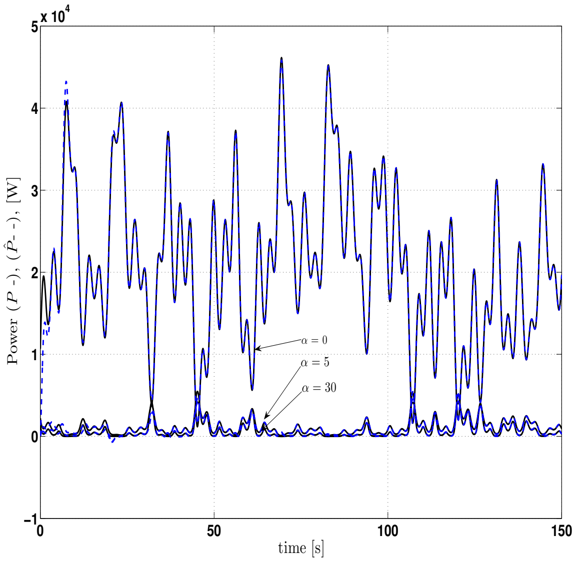

Figure 12. Mechanical power versus time, for the four parameters model. Reference: solid, estimated: dotted. Case 2: $\omega = 6$ and α= 0, 5, 30.

$0, 5, 30$, are shown in Fig. 12. Power estimation is very good and the worst error occurs for $\alpha = 30$, which it is about 1.6%.

Fig. 13 shows the time evolution of the identified parameters, while Fig. 14 illustrates the behavior of the final parameters value with respect to α. The complexity of the curves shape in this case is smaller than in Case 1, although bigger than in the three parameters model case.

5. CONCLUSION

Two new models to represent the available power in a wind turbine were presented. These models were inspired by pseudo-static and dynamic friction model representations in an attempt to reproduce the transformation from kinetic energy in the wind to kinetic energy in the blades as a friction phenomena. The new models made use of a notion of relative velocity between the wind and the blades. They show a similar behavior that one popular heuristic model available in the literature. There are two main advantages in using the new representations: they have a physical interpretation and it is possible to use standard identification techniques to obtain the set of parameter values for a given wind turbine.

Experimental verification of these models is ongoing work. A study of the dependence on the parameters on ω and α,

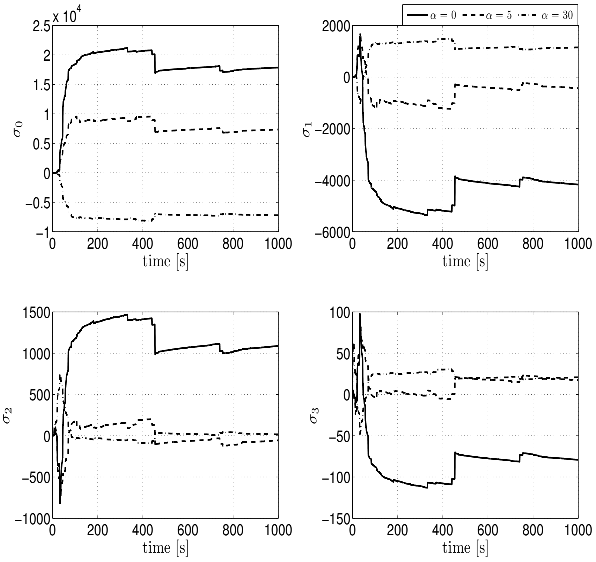

Figure 13. Time evolution of identified parameters for the four parameters model. Case 2: $\omega = 6$ and $\alpha = 0, 5, 30$.

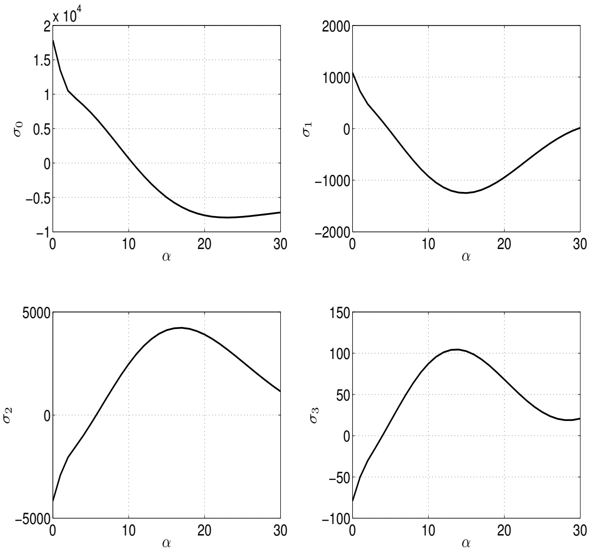

Figure 14. Final parameter estimation versus α for the four parameters model. Case 2: $\omega = 6$.

respectively, that lead to a global model of the available power is also in progress.

REFERENCES

M.J. Balas, A. Wright, M. Hand, and K. Stol. Dynamics and control of horizontal axis wind turbines. In *Proceedings of the 39th IEEE Conference on Decision and Control*, pages 3781–3793, June 2003.

C. Canudas de Wit, H. Olsson, J. Åstrom, and P. Lischinsky. A new model for control of systems with friction. *IEEE Transaction on Automatic Control*, 40(3):419–425, 1995.

A. Dadone and L. Dambrosio. Estimator based adaptive fuzzy logic control technique for a wind turbine-generator system. *Energy Conversion and Management*, 44:135–153, 2003.

Danish. Danish Wind Industry Association. Annual Report of the Danish Wind Industry, March 2003.

S. Heier. *Grid Integration of Wind Energy Conversion Systems*. Wiley, 1998.

Petros A. Ioannou and Jing Sun. *Robust Adaptive Control*. PTR Prentice-Hall, 1996.

M.L. Lima, J.L. Silvino, and P. de Resende. H_∞ control for a variable-speed adjustable-pitch wind energy conversion system. In *Proceedings of the IEEE International Symposium on Industrial Electronics*, pages 556–561, July 1999.

Z. Lin and G. Qingding. Adjustable-pitch and variable-speed control of wind turbines using non linear algorithm. In *Sixth International Conference on Electrical Machines and Systems*, pages 270–273, November 2003.

Y.D. Song, B.Dhinakara, and X.Bao. Control of wind turbines using nonlinear adaptive field excitation algorithms. In *Proceedings of the American Control Conference*, pages 1551–1555, June 2000.

J. Yi, L. Alvarez, and R. Horowitz. Adaptive emergency braking control with underestimation of friction coefficient. *IEEE Transactions on Control Systems Technology*, 10:381–392, 2002.